Published in final edited form as:

J Immunol. 2019 February 01; 202(3): 760–769. doi:10.4049/jimmunol.1801187.

SRC3 is a co-factor for RORγt in Th17 differentiation but not thymocyte development

Zhiheng He[*], **Jing Zhang**[*,†], **Qian Du**[*], **Jianming Xu**[1], **Yousang Gwack**[‡], and **Zuoming Sun**[*]

[*]Department of Molecular Immunology, Beckman Research Institute of the City of Hope, Duarte, CA, 91010

[†] Irell & Manella Graduate School of Biological Sciences, City of Hope, Duarte, CA, 91010

[1]Department of Molecular & Cellular Biology, Baylor College of Medicine, Houston, TX, 77030 United States

[‡]Department of Physiology, David Geffen School of Medicine, UCLA, Los Angeles, CA, 90095

Abstract

SRC3, a highly conserved member of the steroid receptor co-activator (SRC) family, is recruited by transcription factors to regulate cellular function. Previously, we demonstrated that SRC1, another highly conserved member of SRC family, interacts with RORγt to regulate of Th17 differentiation. However, the relationship between SRC1 and SRC3 in the regulation of Th17 cell function remains unknown. Here, we demonstrate that mouse SRC3 interacts with RORγt in Th17 cells but not in thymocytes. In addition, *Src3*$^{-/-}$ mice exhibited defective Th17 differentiation and induction of experimental autoimmune encephalomyelitis but normal thymocyte development. Furthermore, a lysine 313 to arginine mutation of RORγt (RORγt-K313R), which disrupts the interaction of RORγt with SRC3 but not with SRC1, impairs Th17 differentiation but not thymocyte development. These data suggest that SRC3 works with SRC1 to regulate RORγt-dependent Th17 differentiation but is not essential for RORγt-dependent thymocyte development.

Introduction

The transcription factor RORγt directs the differentiation of Th17 cells, which secrete IL-17 (1). Th17 cells participate in protective immunity but also mediate pathological immune responses involved in autoimmune conditions, such as multiple sclerosis, colitis, and autism. Thus, inhibiting Th17 cell formation and function may prevent the development and progression of these conditions (2–7). Because RORγt is required for the generation of pathogenic Th17 cells, it is an attractive drug target for controlling Th17-mediated immunological disorders (8, 9). However, mice deficient in RORγt have been found to exhibit severe defects in thymocyte development, including thymocyte apoptosis, abnormal cell cycle progression, and accumulation of immature CD8^{+} cells (10, 11). Thus, broadly targeting RORγt could lead to severe unintended side effects. To develop more targeted

Address correspondence and reprint requests to: Zuoming Sun, Department of Molecular Immunology, Beckman Research Institute, City of Hope, 1500 East Duarte Road, Duarte, CA 91010, Phone: 626-256-4673, Fax: 626-256-6415 zsun@coh.org.

approaches to inhibit Th17 differentiation, it is important to understand the mechanisms regulating RORγt activity.

Transcription factors like RORγt, which belongs to the steroid nuclear receptor family (11), cannot regulate cellular function unless in the presence of co-factors. Co-factors do not usually have DNA-binding activity and thus depend on transcription factors to carry them to the chromatin to regulate gene expression. The highly conserved steroid receptor co-activator (SRC) family consists of three members, SRC1, SRC2, and SRC3, which are important co-factors for steroid nuclear receptor-mediated transactivation. The SRCs recruit acetyltransferases and methyltransferases that epigenetically modify histones to activate gene expression (12). Our previous study showed that RORγt recruits SRC1 to stimulate Th17 differentiation (13). However, mice deficient in SRC1 only show partially impaired Th17 differentiation (13). Furthermore, it was reported recently that SRC3 also regulates Th17 differentiation (14). The highly conserved nature of the SRC family led us to question the relationship between SRC1 and SRC3 in the function of Th17 cells.

In this study, we demonstrate that SRC3 is a co-factor for RORγt that is necessary for Th17 differentiation but not for thymic T cell development. We detected SRC3-RORγt complexes in Th17 cells but not in thymocytes. In addition, $CD4^+$ T cells from *Src3*$^{-/-}$ mice exhibited defective Th17 differentiation and induction of passive experimental autoimmune encephalomyelitis (EAE) after adoptive transfer. In contrast, *Src3*$^{-/-}$ mice did not exhibit the defects in thymocyte development observed in RORγt-deficient mice. Furthermore, we identified a lysine to arginine mutation in RORγt (RORγt-K313R) that specifically disrupts the interaction between RORγt and SRC3 but not SRC1. Cells expressing RORγt-K313R exhibited impaired Th17 differentiation but normal thymocyte development. Therefore, whereas RORγt must interact with SRC3 to regulate Th17 differentiation, the SRC3-RORγt interaction is not essential for RORγt-regulated thymocyte development.

Materials & Methods

Mice

The *Rorγt*$^{-/-}$ (*Rorc2*$^{-/-}$) and *Src3*$^{-/-}$ mouse strains, described previously (10, 15), were bred and housed under specific pathogen-free conditions in the Animal Resource Center at the Beckman Research Institute of City of Hope under protocols approved by the Institutional Animal Care and Use Committee. Mice were 10–12 weeks of age for EAE and 6–8 weeks for all other experiments, with littermates age-matched across experimental groups.

Antibodies, cytokines and plasmids

Antibodies against RORγt (Q31–378, BD Bioscience), SRC1 (128E7, Cell Signaling), SRC3 (ab2831, Abcam), and FLAG (M2, Sigma-Aldrich) were used for immunoblot analysis. PE-indotricarbocyanine (Cy7)-conjugated anti-CD8 (53–6.7), PE-conjugated anti-RORγt (B2D), allophycocyanin (APC)-conjugated anti-IL-17A (eBio17B7), PE-conjugated anti-Thy1.2 (53–2.1), PE-conjugated anti-CD24 (M1/69), PE-conjugated anti-TCRβ (H57–597), PE-Cy5-conjugated anti-CD19 (eBio1D3), PE-conjugated anti-CD11b (M1/70), FITC-conjugated anti-CD4 (GK1.5), APC-conjugated anti-IL-4 (11B11), and APC-conjugated

anti-Foxp3 (FJK-16s) were from eBioscience. Monoclonal antibodies against mouse CD3 (145–2C11), CD28 (37.51), IL-4 (11B11), IFNγ (XMG1.2), and the p40 subunit of IL-12 and IL23 (C17.8), as well as PE-Cy7-conjugated anti-Ly6G (1A8), FITC-conjugated anti-IFNγ (XMG1.2), PE-conjugated anti-GM-CSF (MP1–22E9), FITC-Cy7-conjugated anti-CD45 (104), and PE-conjugated anti-CD25 (PC61.5) were purchased from Biolegend. Goat anti-hamster antibody was from MP Biomedicals. APC-conjugated anti-CD3 (145–2C11) and FITC-conjugated anti-CD44 (IM7) were from BD Pharmingen. Recombinant mouse IL-12, IL-4, IL-6, IL-23, and TGFβ were from Miltenyi Biotech. An empty retroviral expression plasmid murine stem cell virus (MSCV)-IRES-GFP and those encodes RORγt and SRC1 have been described previously (13). Mouse SRC3 was amplified and inserted into pMSCV-IRES-GFP. Point mutations of RORγt were generated using a site-directed mutagenesis kit from Agilent Technologies.

Retrovirus Transduction

Platinum-E retroviral packaging cells (Cell Biolabs) were plated in a 10-cm dish in 10 ml RPMI-1640 medium plus 10% FBS. 24 h later, cells were transfected with an empty pMSCV vector or the appropriate retroviral expression plasmids with BioT transfection reagent (Bioland). After overnight incubation, the medium was replaced and cultures were maintained for another 24 h. Viral supernatants were collected 48 h and 72 h later, passed through 0.4-μm filters (Millipore), and supplemented with 8 μg/ml of polybrene (Sigma-Aldrich) and 100 U/ml of recombinant IL-2 (for transducing $CD4^+$ T cells) or 5 ng/ml of recombinant IL-7 (for transducing $CD4^-CD8^-$ thymocytes). Naïve $CD4^+$ T cells were first activated with 0.25 μg/ml hamster anti-CD3 (145–2C11; Biolegend) and 1 μg/ml hamster anti-CD28 (37.51; Biolegend) in 24-well plates pre-coated with 0.2 mg/ml goat anti-hamster antibody for 24 h, then spin-infected with viral supernatants (1200 g, 30°C for 2 h). The retroviral supernatant was also used to infect $CD4^-CD8^-$ thymocytes that had been co-cultured with feeder OP9-DL4 cells (a generous gift from Dr. Ellen Rothenberg, Caltech) in the presence of recombinant IL-7 (5 ng/ml) for 24 h. After spin infection, viral supernatant was replaced with culture media containing polarizing cytokines for *in vitro* differentiation (for transduced CD^+ T cells) or 5 ng/ml of recombinant IL-7 for *in vitro* T cell development (for transduced $CD4^-CD8^-$ thymocytes), as described below.

In vitro differentiation

Naïve $CD4^+$ T cells were purified from C57BL/6, $Ror\gamma t^{-/-}$, $Src3^{+/-}$, or $Src3^{-/-}$ mice by negative selection (Miltenyi Biotec). Suspensions of 4×10^5 cells/ml Iscove's modified DMEM (Cellgro) containing 2 mM L-glutamine, 50 mM 2-ME, 100 U/ml penicillin, 100 mg/ml streptomycin, and 10% FBS were cultured in 24-well plates pre-coated with 0.2 mg/ml goat anti-hamster antibody for three days. The medium was supplemented with 0.25 μg/ml hamster anti-CD3, 1 μg/ml hamster anti-CD28, and polarizing cytokines: 2 ng/ml TGFβ, 20 ng/ml IL-6, 5 μg/ml anti-IL-4, and 5 μg/ml anti-IFNγ for Th17 differentiation; 20 μg/ml IL-12 and 5 μg/ml anti-IL-4 for Th1 differentiation; 10 ng/ml IL-4 and 10 μg/ml anti-IFNγ for Th2 differentiation; or 5 ng/ml TGFβ for Treg differentiation. For analysis, cells obtained from *in vitro* cultures were incubated for 4–5 h with 50 ng/ml PMA (Sigma-Aldrich), 750 ng/ml ionomycin (Sigma-Aldrich), and 10 μg/ml brefeldin A (BD Biosciences) in an incubator at 37°C, followed by intracellular cytokine staining.

In vitro T cell development

Thymocytes were stained with 7-AAD and antibodies against Thy1.2, CD4, and CD8. Specific 7-AAD$^-$Thy1.2$^+$CD4$^-$CD8$^-$ populations were sorted using a FACSAria (BD Biosciences) and cultured at 5×10^5/ml overnight on an 80% confluent OP9-DL4 monolayer in a flat-bottom 24-well culture plates with αMEM (MEM α medium; Invitrogen Life Technologies) supplemented with 20% FBS, 100 U/ml penicillin-streptomycin, 2 mM L-glutamine (Invitrogen Life Technologies), and 5 ng/ml recombinant murine IL-7. After 72 h, co-cultures were harvested for flow cytometry analysis.

Flow cytometry

Mouse thymi were homogenized by crushing with the head of a 1-ml syringe in a petri dish, followed by straining through a 40-μm nylon filter. Red Blood Cell Lysing buffer (Sigma-Aldrich) was used for red cell lysis. Cells isolated from thymi, co-cultures harvested from *in vitro* development, and CD4$^+$ T cells stimulated appropriately were stained for surface markers. Intracellular cytokines was stained with Fixation/Permeabilization solution (BD Cytofix/Cytoperm Kit; BD Biosciences). The expression of surface and intracellular markers was analyzed BD FACSCanto flow cytometry system (BD).

RNA sequencing and analysis

To assess the gene expression profile of Th17 cells, naive CD4$^+$ T cells were polarized under Th17 conditions for three days. RNA was isolated using an miRNeasy Mini Kit (Qiagen). Quality verification, library preparation, and sequencing were performed in the City of Hope Integrative Genomics Core facility. Eluted RNAs were prepared for sequencing using Illumina protocols and sequenced on an Illumina HiSeq 2500 to generate 51-bp reads. Sequenced reads were aligned to the mouse mm10 reference genome using TopHat. Gene expression levels were quantified by HTSeq, and edgeR was utilized to identify differentially expressed genes (fold-change > 1.5 and FDR < 0.05). Gene expression abundance was quantified as fragments per kilobase of transcript per million fragments mapped (FPKM). Heat maps of differentially expressed genes were made using gplots with log2-transformed FPKM values.

Chromatin immunoprecipitation

2×10^7 cells were incubated with 1% formaldehyde for 5 min at room temperature to cross-link proteins with chromatin. 125 mM glycine was added to stop the cross-linking reaction. To shear genomic DNA into 200–500-bp fragments, cell lysates were sonicated using a water-bath sonicator (Covaris S200). Cell lysates were centrifuged (12000 g, 10 min) and incubated with specific antibodies or IgG controls and protein A/G beads (Millipore). After extensive washing, DNA was eluted, followed by reversion of the protein–DNA cross-linking. DNA was recovered for qRT-PCR to quantify specific DNA fragments that were precipitated.

qRT-PCR

qRT-PCR was performed using SsoFast EvaGreen Supermix (Bio-Rad) in a CFX96 Real-Time PCR Detection System (Bio-Rad) using primers as following: Il17a-F:

TTTAACTCCCTTGGCGCAAAA, Il17a -R:CTTTCCCTCCGCATTGACAC; Il17f -F: TGCTACTGTTGATGTTGGGAC, Il17f -R: AATGCCCTGGTTTTGGTTGAA; Ccr6-F: CCTGGGCAACATTATGGTGGT, Ccr6-R: CAGAACGGTAGGGTGAGGACA; Ccl20-F: GCCTCTCGTACATACAGACGC, Ccl20-R: CCAGTTCTGCTTTGGATCAGC; Irf4-F: TCCGACAGTGGTTGATCGAC, Irf4-R: CCTCACGATTGTAGTCCTGCTT; Rora-F: GTGGAGACAAATCGTCAGGAAT, Rora-R: TGGTCCGATCAATCAAACAGTTC; Ahr-F: AGCCGGTGCAGAAAACAGTAA, Ahr-R: AGGCGGTCTAACTCTGTGTTC. Conditions were adjusted to optimize primer amplification efficiency for all qRT-PCR reactions. Expression was calculated using the ΔΔct method and normalized to *β-actin*. All measurements were performed in triplicate.

Apoptosis assays

Thymocytes were freshly isolated and cultured in RPMI 1640 medium supplemented with 10% FBS, 100 U/ml penicillin-streptomycin, and 2 mM L-glutamine at 1×10^6 cells/ml. Thymocytes were incubated at 37°C with 5% CO_2. Dead cells were detected using Annexin V-PE and 7-AAD staining (BD Bioscience).

Induction and assessment of experimental autoimmune encephalomyelitis (EAE)

For Th17-induced passive EAE, donor mice were subcutaneously immunized with a 200-μg myelin oligodendrocyte glycoprotein 35–55 ($MOG_{35–55}$) peptide emulsion (Hooke Laboratories, Lawrence, MA). 10 days later, cells were isolated from the spleen and lymph nodes and cultured with 20 μg/ml $MOG_{35–55}$ for 3 days under Th17-polarizing conditions (20 ng/ml recombinant mouse IL23). $Src3^{+/-}$ recipient mice were then intraperitoneally transferred 3.0×10^7 $MOG_{35–55}$-specific Th17 cells. The severity of EAE was monitored and evaluated on a scale from 0 to 5, according to guidelines from the Hooke Laboratories: 0 = no disease; 1 = paralyzed tail; 2= hind limb weakness; 3= hind limb paralysis; 4 = hind and fore limb paralysis; 5= moribund and death. When a mouse was euthanized because of severe paralysis, a score of 5 was entered for that mouse for the rest of the experiment.

Immunoprecipitation and immunoblot analysis

Cells were lysed in lysis buffer (1% Triton X-100, 20 mM Tris-cl, pH 7.4, 150 mM NaCl, and 5 mM EDTA) supplemented with protease inhibitor cocktail (Sigma) and 1 mM PMSF. Cell extracts were incubated overnight with 1 μg of the relevant antibodies, and proteins were immunoprecipitated for an additional 1 h at 4°C with protein A/G-Sepharose beads (Millipore). After incubation, beads were washed four times with lysis buffer, resolved using SDS-PAGE, and analyzed using Western blot.

Statistical analysis

GraphPad Prism software was used for all statistical analyses. Two-tailed, unpaired Student's t tests and one-way analysis of variance (ANOVA) were used to compare experimental groups. A *P* value of less than 0.05 was considered statistically significant.

Results

SRC3 interacts with RORγt in Th17 cells but not in thymocytes.

Mass spectrometric analysis of RORγt-binding proteins in Th17 cells detected both SRC1 and SRC3 (data not shown), which was confirmed by immunoprecipitation assay using HEK293T cells expressing RORγt and SRC1 or SRC3 (Fig. 1A). This was consistent with our previous finding that RORγt recruits SRC1 to regulate Th17 differentiation (13). We next monitored the interactions between RORγt and SRC3 in both Th17 cells and thymocytes, in which RORγt is known to play important roles (11). Whereas SRC1 was found to interact with RORγt in both mouse Th17 cells and thymocytes (Fig. 1B), the SRC3-RORγt interaction was only detected in Th17 cells (Fig. 1C). RORγt binds to *Il17a* and *Il17f* loci to stimulate their expression (11, 16). To determine whether RORγt recruits SRC3 to *Il17a* and *Il17f* loci, we performed a ChIP assay. Consistent with previous results (11), RORγt binding to *Il17a* and Il17f loci was detected in wildtype (WT) but not *RORγt*$^{-/-}$ cells differentiated under Th17 polarization conditions (Fig. 1D and1E). SRC1 is known to bind to the *Il17* gene (17) and thus was used as a positive control. Indeed, both SRC1 and SRC3 were found to bind to *Il17a* and *Il17f* loci in WT Th17 cells, but binding to both loci was significantly reduced in *RORγt*$^{-/-}$ cells, suggesting that RORγt recruits both SRC1 and SRC3 to the *Il17* gene. These results demonstrate that SRC3 interacts with RORγt in Th17 cells but not in thymocytes.

SRC3 regulates Th17 differentiation.

Because SRC3 interacts with RORγt in Th17 cells, we determined whether it plays a role in Th17 differentiation using *Src3*$^{-/-}$ mice. There were no differences in Th17 differentiation of CD4^{+} T cells obtained from WT and *Src3*$^{+/-}$ mice (Supplementary Fig. 1A), therefore we used *Src3*$^{+/-}$ mice as WT controls in this study. We found that Th17 but not Th1 differentiation of CD4^{+} T cells from *Src3*$^{-/-}$ mice was greatly reduced compared to that of CD4^{+} T cells from *Src3*$^{+/-}$ mice (Fig. 2A). However, the RORγt expression in *Src3*$^{-/-}$ T cells was similar to that in *Src3*$^{+/-}$ Th17 cells (Fig. 2B), suggesting that reduced Th17 differentiation is not due to changes in RORγt expression but likely due to reduced RORγt activity in the absence of SRC3. Furthermore, expression of critical Th17 genes, including *Il17a*, *Il17f*, *Ccr6*, and *Ccl20,* but not *Il23r, Ahr*, and *Irf4*, were reduced in *Src3*$^{-/-}$ T cells (Fig. 2C and Supplementary Fig. 1B), suggesting severe impairment of the Th17 differentiation program. We next performed a ChIP assay to detect the binding of SRC3 to different gene loci; SRC1 was used as a positive control, as it is known to bind *Il17a* and *Il17f* loci (17). We found that SRC3 binding to the *Il23r* locus is significantly lower than its binding to *Il17a* and *Il17f* loci (Fig. 2D). This difference in binding correlated with the differences in expression *Il17a*, *Il17f*, and *Il23r* (Fig. 2C), indicating the contribution of SRC3 to the expression of the IL-17 gene.

Because SRC1 and SRC3 are highly conserved and both regulate Th17 differentiation, we examined whether SRC1 can compensate for deficient SRC3 function in Th17 differentiation. First, we found that the SRC1-RORγt interaction in Th17 cells was not affected by the absence of SRC3 (Fig. 2E). Furthermore, SRC3 but not SRC1 could rescue

Th17 differentiation in *Src3*$^{-/-}$ T cells (Fig.2F), suggesting that the function of SRC3 does not overlap with that of SRC1 in the regulation of Th17 differentiation.

T cells from *Src3*$^{-/-}$ mice are defective in the induction of EAE.

To determine whether SRC3 plays a role in pathogenic Th17 immunity, we examined the effects of SRC3 deficiency on Th17 differentiation under pathogenic conditions. Under normal conditions (i.e., in the presence of TGFβ + IL-6), the Th17 differentiation of *Src3*$^{-/-}$ T cells was impaired compared to that of *Src3*$^{+/-}$ T cells. This difference was even more severe for Th17 differentiation under pathogenic conditions (IL-6 + IL-1 + IL-23) (Fig. 3A). Consistent with this observation, we also observed that the downregulation of critical Th17 genes, including *Il7a, Il7f, Il22, Il1r1, Rora,* and *Il23r,* but not *Rorc,* in *Src3*$^{-/-}$ T cells was greater under pathogenic conditions than under normal conditions (Supplementary Fig. 1C). Despite the significant effects of SRC3 deficiency, overexpression of SRC3 did not significantly affect *Il1r1* expression (Supplementary Fig. 1D). We next tested the function of *Src3*$^{-/-}$ T cells in the induction of pathogenic EAE after adoptive transfer. Indeed, CD4$^+$ T cells from *Src3*$^{-/-}$ mice polarized under Th17 conditions induced much less severe EAE compared to control CD4$^+$ T cells from *Src*$^{+/-}$ mice (Fig. 3B). The reduced induction of EAE correlated with reduced central nervous system (CNS) infiltration by different kinds of lymphocytes, including Ly6G$^+$ neutrophils, CD4$^+$ and CD8$^+$ T cells, CD19$^+$ B cells, and CD11b$^+$ monocytes, an indication of less inflammation (Fig. 3C and3D). In addition, we observed reduced expression of critical Th17 genes, *IL17a, Il17f, Csf2, Il22*, *Cxcr3*, and *Ccl20*, in CNS-infiltrating lymphocytes recovered from mice adoptively transferred with *Src3*$^{-/-}$ CD4$^+$ T cells (Fig. 3E). These results demonstrate that SRC3 is required for Th17-mediated EAE.

SRC3 is not required for thymocyte development.

In addition to Th17 differentiation, RORγt regulates thymocyte development. *RORγt*$^{-/-}$ mice had greater numbers of immature CD8$^+$ cells and larger thymocytes that exhibited accelerated apoptosis and abnormal S phase entry (10, 18). Since SRC3 is required for RORγt-regulated Th17 differentiation, we examined whether SRC3 also plays a role in thymocyte development. There were no differences between *Src3*$^{-/-}$ mice and control *Src3*$^{+/-}$ mice in the expression of RORγt (Fig. 4A) or the size of thymocytes (Fig. 4B). Furthermore, flow cytometric analysis of surface CD4 and CD8 markers indicated that the percentages (Fig. 4C) and numbers (Fig. 4D) of CD4$^-$CD8$^-$, CD4$^+$CD8$^+$, and CD4$^+$ and CD8$^+$ cells, three sequential developmental stages of thymocytes, were also normal. We also did not observe increased percentages (Fig. 4E) and numbers (Fig. 4F) of immature CD8$^+$ (i.e., CD4$^+$CD24^{hi}TCRβ^{lo}) cells in *Src3*$^{-/-}$ mice (Fig. 4E); differences in the number of cells with more than 2N DNA (Fig. 4F); or reduced thymocyte survival (Fig. 4G) in the absence of SRC3. RORγt is thought to control cell cycle progression and the survival of thymocytes by stimulating the expression of Bcl-x$_L$ (*Bcl2l1*), as overexpression of Bcl-x$_L$ prevents abnormal cell cycle progression and apoptosis in *RORγt*$^{-/-}$ thymocytes (10). Consistent with our findings that suggest that SRC3 does not play a role in RORγt-regulated cell cycle and survival during thymocyte development, we did not detect changes in the expression of *Bcl2l1* in *Src3*$^{-/-}$ thymocytes (Fig. 4H). Lastly, we observed no differences in the differentiation of CD4$^-$CD8$^-$ thymocytes from *Src3*$^{-/-}$ and *Src*$^{+/-}$ mice *in vitro* on stromal

cells (Fig. 4I). Taken together, these data suggest that SRC3 is not required for RORγt-dependent thymocyte development.

Disruption of the RORγt-SRC3 interaction impairs RORγt function in Th17 differentiation but not thymocyte development.

To separate the functions of the RORγt-SRC3 and RORγt-SRC1 interactions, we created an RORγt mutant that can bind SRC1 but not SRC3. To do this, we systematically mutated amino acids in RORγt that are predicted to contact SRCs, based on the X-ray structure of an SRC peptide-RORγt complex (Supplementary Fig. 1E) (19). Among the RORγt mutants, only the lysine 313 to arginine mutation (RORγt-K313R) significantly impaired the interaction of RORγt with SRC3 but did not affect the RORγt-SRC1 interaction (Fig. 5A and5B). We next tested the function of RORγt-K313R by introducing it retrovirally into *RORγt*$^{-/-}$ cells. Unlike WT RORγt, RORγt-K313R could not restore Th17 differentiation in *RORγt*$^{-/-}$ CD4^{+} cells (Fig. 5C) but could rescue thymocyte development in *RORγt*$^{-/-}$ thymocytes (Fig. 5D). *RORγt*$^{-/-}$ CD4^{+} cells reconstituted with RORγt-K313R also exhibited reduced expression of critical Th17 genes including *Il17a*, *Il17f*, *Il22*, *Ccl20*, and *Ccr6*, confirming the inability of RORγt-K313R to support Th17 differentiation (Fig. 5E and Supplementary Fig.1F). Furthermore, we conducted a ChIP assay using *RORγt*$^{-/-}$ CD4^{+} cells and found that RORγt-K313R had impaired affinity for both *Il17a* and *Il17f* loci compared to WT RORγt (Fig. 5F). Altogether, these data indicate that the RORγt-SRC3 interaction is essential to regulate Th17 differentiation but dispensable for thymocyte development.

Discussion

SRC3 has long been known to be a co-factor for nuclear receptors, and it was recently found to be required for pathogenic Th17 immunity responsible for the development of EAE (14). Here, we confirmed these findings and furthermore demonstrated that SRC3 works non-redundantly with SRC1 in Th17 differentiation. Although Tanaka et al. reported that SRC3 is necessary only for pathogenic Th17 immunity, we observed defective Th17 differentiation even under normal differentiation conditions (TGFβ + IL-6). This discrepancy may be due to our use of constitutive SRC3 knockout mice instead of conditional SRC3 knockout mice (14), which likely caused developmental changes in T cells. Nevertheless, both studies support the importance of SRC3 in pathogenic Th17 immunity. We also found that *Src3*$^{-/-}$ mice have normal thymic T cell development. Specifically, we demonstrated that SRC3 interacts with RORγt in Th17 cells but not in thymocytes and disruption of the RORγt-SRC3 interaction impairs its function in Th17 differentiation but not thymocyte development.

As members of the same co-activator family, SRC1 and SRC3 are highly conserved and both interact with RORγt to stimulate Th17 differentiation, indicating that they have similar functions in Th17 cells. However, deficiency in either SRC1 or SRC3 leads to defective Th17 differentiation and Th17-dependent development of EAE (17), and thus SRC1 and SRC3 non-redundantly regulate Th17 function. Furthermore, the RORγt-K313R mutant that binds SRC1 but not SRC3 failed to fully restore Th17 differentiation in *RORγt*$^{-/-}$ T cells.

These results suggest that the function of SRC1 and SRC3 do not overlap in the regulation of Th17 differentiation and T cell-mediated Th17 immunity. Our data suggest two potential mechanisms responsible for the distinct roles of SRC1 and SRC3 in Th17 cells. First, some DNA-binding sites may preferentially bind SRC1 or SRC3. Second, some genes may be regulated by both SRC1 and SRC3, whereas others are regulated by only one.

Why SRC3 is necessary as a co-factor for RORγt in Th17 cells but not in thymocytes is not understood. However, we observed that RORγt interacts with SRC3 in Th17 cells but not in thymocytes, suggesting that RORγt selectively recruits SRC3 in Th17 cells and uses different co-factors in thymocytes. Its co-factors in thymocytes remain unknown. One apparent candidate is SRC1; however, mice deficient in SRC1 have no obvious defects in thymocyte development (17), suggesting that SRC1, like SRC3, is dispensable for thymocyte development. It would thus be worthwhile to identify additional RORγt co-factors in thymocytes.

Th17 cells produce effector cytokines to mediate the pathological inflammation responsible for many types of autoimmune diseases; targeting Th17 cells is thus a potentially valuable treatment for these diseases (20). Indeed, inhibiting the Th17 pathway is effective for treating psoriasis and multiple sclerosis (21, 22). Given the essential function of RORγt in Th17 cells, pharmaceutical and academic scientists are developing RORγt inhibitors for treatment of Th17-dependent autoimmunity (6, 8, 9, 23, 24). Unfortunately, such RORγt inhibitors can induce thymic lymphoma due to inhibition of RORγt in thymocyte development (25). Although SRC3 is required for Th17 differentiation, it is not essential for regulating thymocyte development (25, 26); therefore, drugs that specifically disrupt the interaction between RORγt and SRC3 are expected to inhibit Th17-mediated pathological immunity without causing lymphoma by interference of thymocyte development. We showed that K313 of RORγt is critical for binding to SRC3, indicating that amino acids surrounding K313 can potentially be targeted to disrupt the RORγt-SRC3 interaction. Therefore, in addition to further investigating a novel function of SRC3 in RORγt-regulated Th17 differentiation, our results also facilitate the development of a new category of RORγt-based drugs that treat Th17-mediated autoimmunity without causing serious side effects.

Supplementary Material

Refer to Web version on PubMed Central for supplementary material.

Acknowledgements

We thank Dr. Jianming Xu (Baylor College of Medicine) for sharing the *Src3* knockout mice and Dr. Ellen Rothenberg for sharing OP9-DL4 cells. We also appreciate help from the City of Hope core facilities, including the Animal Resource Center, Integrative Genomics Core, and Analytical Cytometry Core.

This work was supported by a grant from the National Institutes of Health (R01-AI109644) and institutional pilot funding. In addition, research reported in this publication was supported by the National Cancer Institute under award number P30CA33572, which includes work performed in the Animal Resource Center, Integrative Genomics Core, and Analytical Cytometry Core. The content is solely the responsibility of the authors and does not necessarily represent the official views of the National Institutes of Health.

Abbreviations used in this article:

CNS	central nervous system
EAE	experimental autoimmune encephalomyelitis
SRC	steroid receptor co-activator
WT	wildtype

References

1. Korn T, Bettelli E, Oukka M, and Kuchroo VK. 2009 IL-17 and Th17 Cells. Annual review of immunology 27: 485–517.
2. Lee Y, Awasthi A, Yosef N, Quintana FJ, Xiao S, Peters A, Wu C, Kleinewietfeld M, Kunder S, Hafler DA, Sobel RA, Regev A, and Kuchroo VK. 2012 Induction and molecular signature of pathogenic TH17 cells. Nat Immunol 13: 991–999. [PubMed: 22961052]
3. Codarri L, Gyulveszi G, Tosevski V, Hesske L, Fontana A, Magnenat L, Suter T, and Becher B. 2011 RORgammat drives production of the cytokine GM-CSF in helper T cells, which is essential for the effector phase of autoimmune neuroinflammation. Nat Immunol 12: 560–567. [PubMed: 21516112]
4. El-Behi M, Ciric B, Dai H, Yan Y, Cullimore M, Safavi F, Zhang GX, Dittel BN, and Rostami A. 2011 The encephalitogenicity of T(H)17 cells is dependent on IL-1- and IL-23-induced production of the cytokine GM-CSF. Nat Immunol 12: 568–575. [PubMed: 21516111]
5. Elloso MM, Gomez-Angelats M, and Fourie AM. 2012 Targeting the Th17 pathway in psoriasis. Journal of leukocyte biology 92: 1187–1197. [PubMed: 22962689]
6. Skepner J, Ramesh R, Trocha M, Schmidt D, Baloglu E, Lobera M, Carlson T, Hill J, Orband-Miller LA, Barnes A, Boudjelal M, Sundrud M, Ghosh S, and Yang J. 2014 Pharmacologic inhibition of RORgammat regulates Th17 signature gene expression and suppresses cutaneous inflammation in vivo. J Immunol 192: 2564–2575. [PubMed: 24516202]
7. Choi GB, Yim YS, Wong H, Kim S, Kim H, Kim SV, Hoeffer CA, Littman DR, and Huh JR. 2016 The maternal interleukin-17a pathway in mice promotes autism-like phenotypes in offspring. Science 351: 933–939. [PubMed: 26822608]
8. Xiao S, Yosef N, Yang J, Wang Y, Zhou L, Zhu C, Wu C, Baloglu E, Schmidt D, Ramesh R, Lobera M, Sundrud MS, Tsai PY, Xiang Z, Wang J, Xu Y, Lin X, Kretschmer K, Rahl PB, Young RA, Zhong Z, Hafler DA, Regev A, Ghosh S, Marson A, and Kuchroo VK. 2014 Small-molecule RORgammat antagonists inhibit T helper 17 cell transcriptional network by divergent mechanisms. Immunity 40: 477–489. [PubMed: 24745332]
9. Huang Z, Xie H, Wang R, and Sun Z. 2007 Retinoid-related orphan receptor gamma t is a potential therapeutic target for controlling inflammatory autoimmunity. Expert opinion on therapeutic targets 11: 737–743. [PubMed: 17504012]
10. Sun Z, Unutmaz D, Zou YR, Sunshine MJ, Pierani A, Brenner-Morton S, Mebius RE, and Littman DR. 2000 Requirement for RORgamma in thymocyte survival and lymphoid organ development. Science 288: 2369–2373. [PubMed: 10875923]
11. He Z, Ma J, Wang R, Zhang J, Huang Z, Wang F, Sen S, Rothenberg EV, and Sun Z. 2017 A two-amino-acid substitution in the transcription factor RORgammat disrupts its function in TH17 differentiation but not in thymocyte development. Nat Immunol 18: 1128–1138. [PubMed: 28846085]
12. Walsh CA, Qin L, Tien JC, Young LS, and Xu J. 2012 The function of steroid receptor coactivator-1 in normal tissues and cancer. International journal of biological sciences 8: 470–485. [PubMed: 22419892]
13. Sen S, Wang F, Zhang J, He Z, Ma J, Gwack Y, Xu J, and Sun Z. 2018 SRC1 promotes Th17 differentiation by overriding Foxp3 suppression to stimulate RORgammat activity in a PKC-theta-

dependent manner. Proceedings of the National Academy of Sciences of the United States of America 115: E458–E467. [PubMed: 29282318]

14. Tanaka K, Martinez GJ, Yan X, Long W, Ichiyama K, Chi X, Kim BS, Reynolds JM, Chung Y, Tanaka S, Liao L, Nakanishi Y, Yoshimura A, Zheng P, Wang X, Tian Q, Xu J, O'Malley BW, and Dong C. 2018 Regulation of Pathogenic T Helper 17 Cell Differentiation by Steroid Receptor Coactivator-3. Cell reports 23: 2318–2329. [PubMed: 29791844]
15. Xu J, Liao L, Ning G, Yoshida-Komiya H, Deng C, and O'Malley BW. 2000 The steroid receptor coactivator SRC-3 (p/CIP/RAC3/AIB1/ACTR/TRAM-1) is required for normal growth, puberty, female reproductive function, and mammary gland development. Proceedings of the National Academy of Sciences of the United States of America 97: 6379–6384. [PubMed: 10823921]
16. Ciofani M, Madar A, Galan C, Sellars M, Mace K, Pauli F, Agarwal A, Huang W, Parkurst CN, Muratet M, Newberry KM, Meadows S, Greenfield A, Yang Y, Jain P, Kirigin FK, Birchmeier C, Wagner EF, Murphy KM, Myers RM, Bonneau R, and Littman DR. 2012 A validated regulatory network for Th17 cell specification. Cell 151: 289–303. [PubMed: 23021777]
17. Sen S, Wang F, Zhang J, He Z, Gwack Y, Xu J, and Sun Z. 2017 SRC1 promotes Th17 differentiation by overriding Foxp3 suppression to stimulate RORgammat activity in a PKC-theta dependent manner. Proceedings of the National Academy of Sciences of the United States of America In press.
18. Xie H, Sadim MS, and Sun Z. 2005 RORgammat recruits steroid receptor coactivators to ensure thymocyte survival. J Immunol 175: 3800–3809. [PubMed: 16148126]
19. Stehlin-Gaon C, Willmann D, Zeyer D, Sanglier S, Van Dorsselaer A, Renaud JP, Moras D, and Schule R. 2003 All-trans retinoic acid is a ligand for the orphan nuclear receptor ROR beta. Nat Struct Biol 10: 820–825. [PubMed: 12958591]
20. Yang J, Sundrud MS, Skepner J, and Yamagata T. 2014 Targeting Th17 cells in autoimmune diseases. Trends in pharmacological sciences 35: 493–500. [PubMed: 25131183]
21. Tonel G, Conrad C, Laggner U, Di Meglio P, Grys K, McClanahan TK, Blumenschein WM, Qin JZ, Xin H, Oldham E, Kastelein R, Nickoloff BJ, and Nestle FO. 2010 Cutting edge: A critical functional role for IL-23 in psoriasis. J Immunol 185: 5688–5691. [PubMed: 20956338]
22. Segal BM, Constantinescu CS, Raychaudhuri A, Kim L, Fidelus-Gort R, Kasper LH, and Ustekinumab MSI. 2008 Repeated subcutaneous injections of IL12/23 p40 neutralising antibody, ustekinumab, in patients with relapsing-remitting multiple sclerosis: a phase II, double-blind, placebo-controlled, randomised, dose-ranging study. The Lancet. Neurology 7: 796–804. [PubMed: 18703004]
23. Huh JR, and Littman DR. 2012 Small molecule inhibitors of RORgammat: targeting Th17 cells and other applications. Eur J Immunol 42: 2232–2237. [PubMed: 22949321]
24. Sheridan C 2013 Footrace to clinic heats up for T-cell nuclear receptor inhibitors. Nature biotechnology 31: 370.
25. Guntermann C, Piaia A, Hamel ML, Theil D, Rubic-Schneider T, Del Rio-Espinola A, Dong L, Billich A, Kaupmann K, Dawson J, Hoegenauer K, Orain D, Hintermann S, Stringer R, Patel DD, Doelemeyer A, Deurinck M, and Schumann J. 2017 Retinoic-acid-orphan-receptor-C inhibition suppresses Th17 cells and induces thymic aberrations. JCI Insight 2: e91127. [PubMed: 28289717]
26. Liljevald M, Rehnberg M, Soderberg M, Ramnegard M, Borjesson J, Luciani D, Krutrok N, Branden L, Johansson C, Xu X, Bjursell M, Sjogren AK, Hornberg J, Andersson U, Keeling D, and Jirholt J. 2016 Retinoid-related orphan receptor gamma (RORgamma) adult induced knockout mice develop lymphoblastic lymphoma. Autoimmun Rev 15: 1062–1070. [PubMed: 27491564]

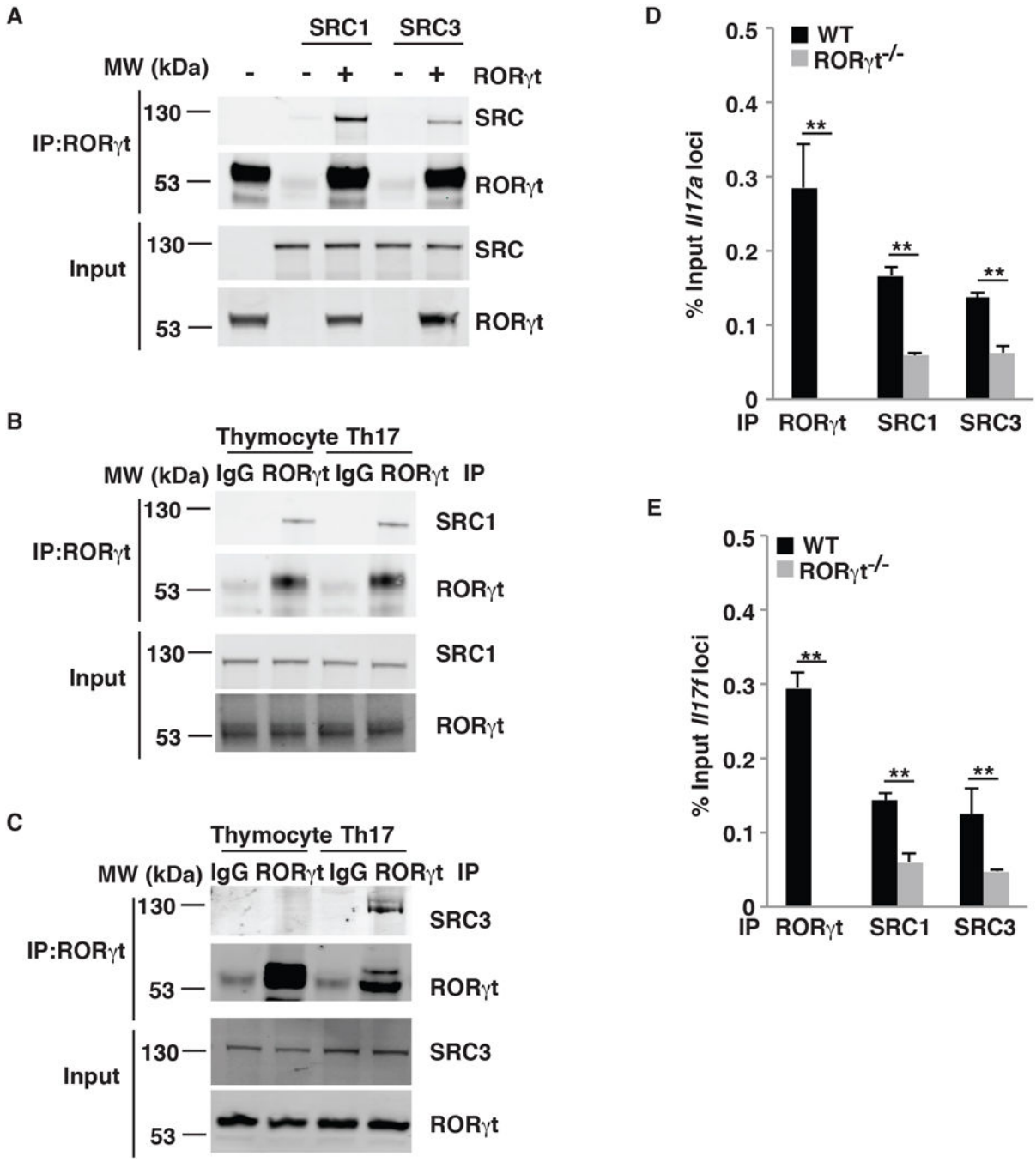

Figure 1.

SRC3 interacts with RORγt in Th17 cells but in not thymocytes. (**A**) Immunoblot analysis of SRC1 and SRC3 immunoprecipitated with an anti-RORγt antibody from HEK293T cells co-transfected with plasmids to express RORγt, SRC1, and/or SRC3. The bottom images show immunoblot analysis of whole-cell lysates without immunoprecipitation (input). (**B**) Immunoblot analysis of SRC1 immunoprecipitated with a control IgG or anti-RORγt antibody from mouse thymocytes and differentiated Th17 cells. (**C**) Immunoblot analysis of SRC3 immunoprecipitated with a control IgG or anti-RORγt antibody from mouse

thymocytes or differentiated Th17 cells. (**D**) ChIP analysis of RORγt, SRC1, and SRC3 bound to the *Il17a* locus in $CD4^+$ T cells from WT or $ROR\gamma t^{-/-}$ mice polarized under Th17 conditions. (**E**) ChIP analysis of RORγt, SRC1, and SRC3 bound to the *Il17f* locus in $CD4^+$ T cells WT or $ROR\gamma t^{-/-}$ mice polarized under Th17 conditions. Data are from one representative of three independent experiments (**A–C**) or are aggregated from three experiments (**D–E**, mean ± SEM). ** P <0.01 (*t-test*).

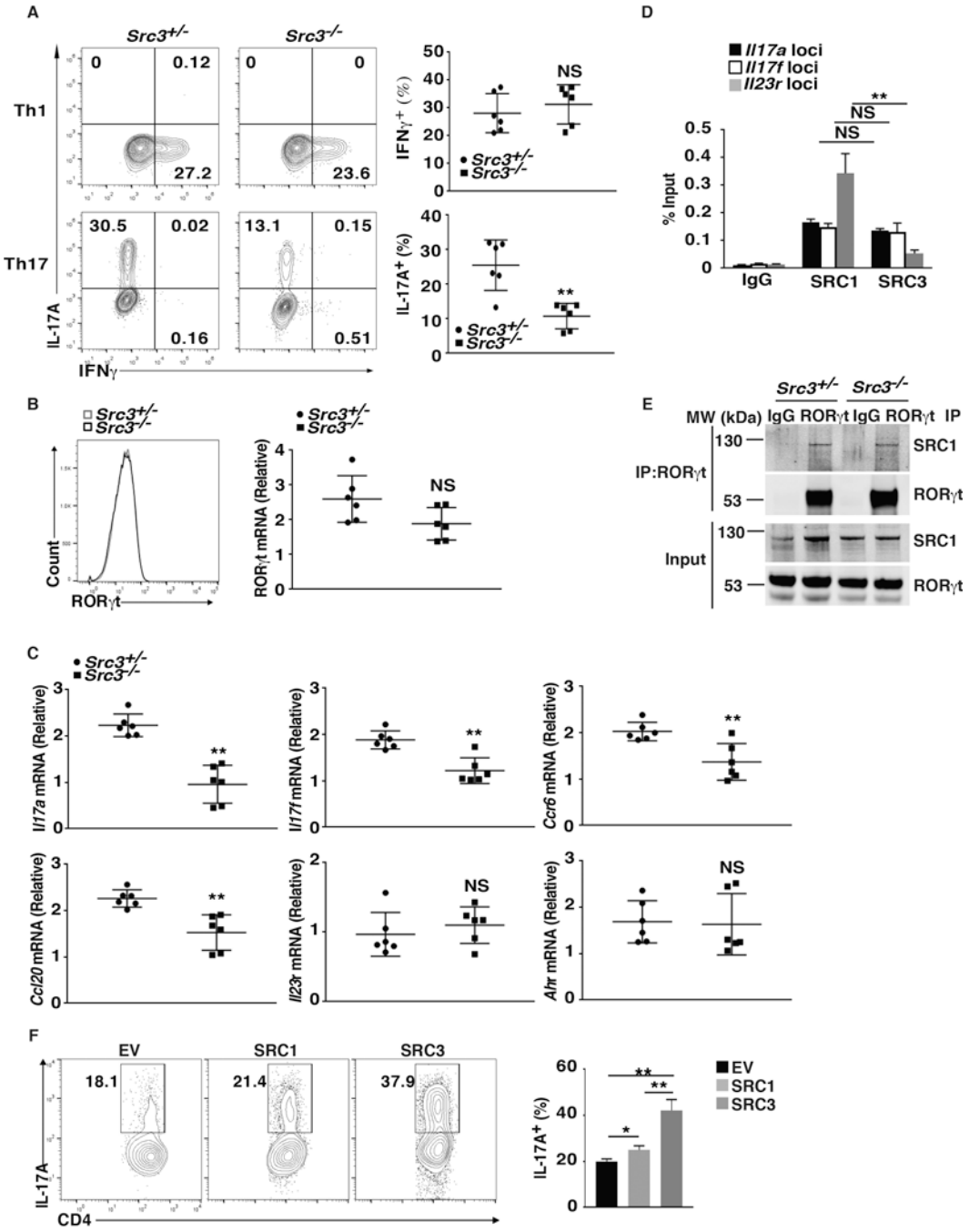

Figure 2.

SRC3 regulates Th17 differentiation. (**A**) Flow cytometric analysis of intracellular IFN**γ** (top panels) and IL-17A (bottom panels) in naïve CD4$^+$ T cells from *Src3*$^{+/-}$ and *Src3*$^{-/-}$ mice, cultured for three days under Th1 or Th17 priming conditions *in vitro* (*n=6* per genotype). Numbers in each plot indicate the percentage of the cells in the gated area. Right panels present the percentages of IFN**γ**$^+$ and IL-17A$^+$ cells from individual mice. (**B**) Flow cytometric analysis of ROR**γ**t levels in naïve CD4$^+$ T cells from *Src3*$^{+/-}$ and *Src3*$^{-/-}$ mice, cultured for three days under Th17 priming conditions *in vitro*. The plot on right shows the

quantification of RORγt mRNA in Th17 cells differentiated from the $CD4^+$ T cells of individual *Src3*$^{+/-}$ and *Src3*$^{-/-}$ mice (*n=6* per genotype). (**C**) qPCR analysis of *Il17a, Il17f, Ccr6, Ccl20, Il23r,* and *Ahr* mRNA in Th17 cells differentiated from the $CD4^+$ T cells of individual *Src3*$^{+/-}$ and *Src3*$^{-/-}$ mice (*n=6* per genotype). (**D**) ChIP analysis of SRC1 and SRC3 binding to *Il17a*, *Il17f*, and *Il23r* loci in $CD4^+$ T cells polarized under Th17 conditions. IgG serves as a negative control. (**E**) Immunoblot analysis of SRC1 immunoprecipitated with a control IgG or anti-RORγt antibody from differentiated *Src3*$^{+/-}$ and *Src3*$^{-/-}$ Th17 cells. (**F**) Flow cytometric analysis of IL-$17A^+$ cells (outlined) among $CD4^+$ T cells from *Src3*$^{-/-}$ mice transduced with a retrovirus expressing GFP alone (EV) or GFP with SRC1 or SRC3 and polarized for three days under Th17 priming conditions. The plot on the right shows the percentages of IL-$17A^+$ cells in each group. Data are aggregated from three experiments (**A** and **B**, right panels; **C**; **D**; **F**; presented as mean ± SEM) or are from one representative of three independent experiments (**E**). NS, not significant (P>0.05); * P < 0.05 (*t-test*); ** P <0.01 (*t-test*).

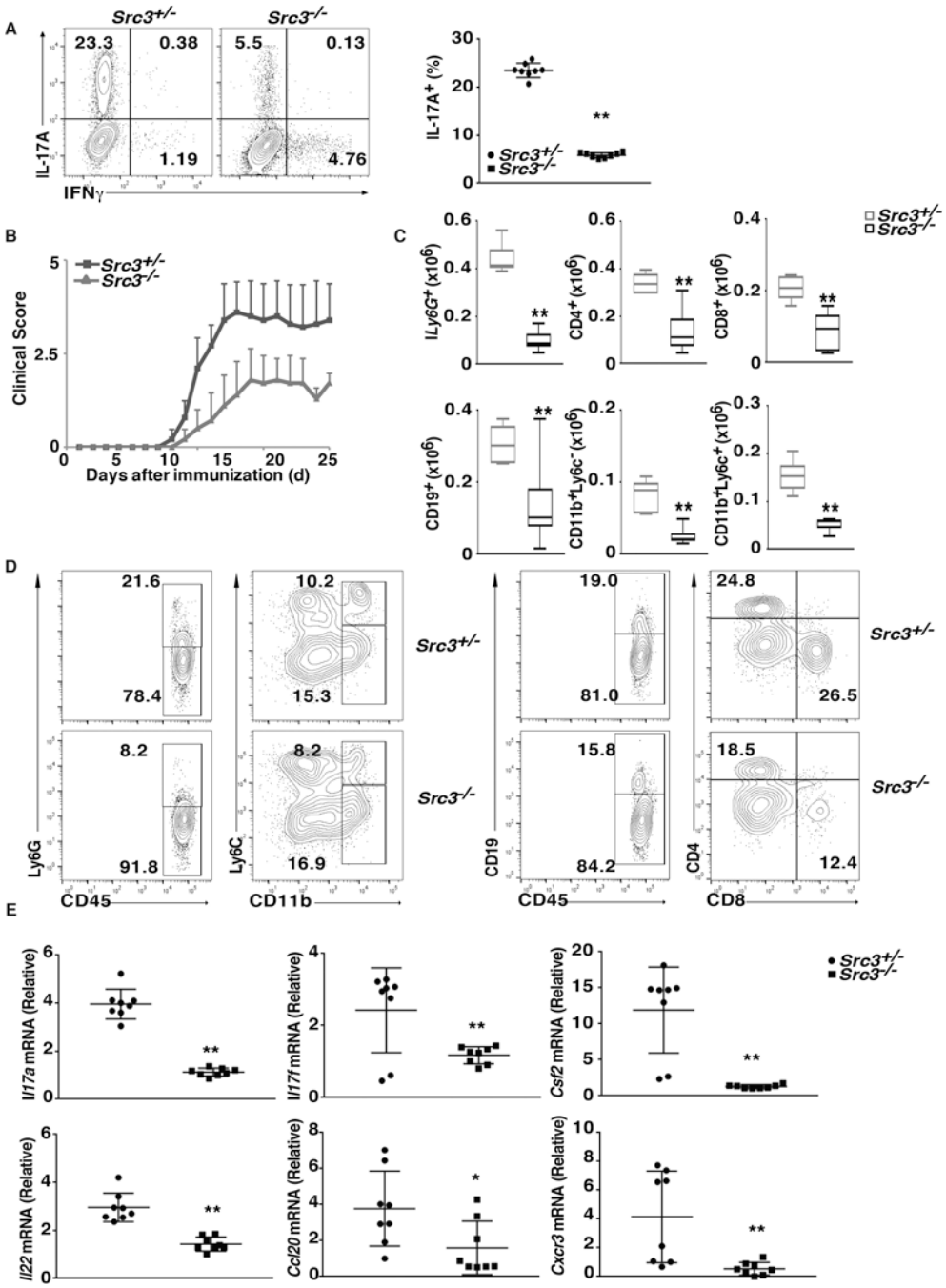

Figure 3.

T cells from *Src3*$^{-/-}$ mice exhibit defective induction of EAE. (**A**) Flow cytometric analysis of intracellular IL-17A in naïve CD4^{+} T cells from *Src3*$^{+/-}$ and *Src3*$^{-/-}$ mice, cultured for three days under pathogenic Th17 priming conditions (TGFβ + IL-6 + IL-1 + IL-23) *in vitro*. Numbers in each plot indicate the percentage of the cells in the gated area. Right panels present the percentages of IL-17A^{+} cells from individual mice (*n=7* per genotype). (**B**) Mean clinical EAE score of *Src3*$^{+/-}$ mice adoptively transferred with CD4^{+} T cells from MOG$_{35–55}$-primed *Src3*$^{+/-}$ or *Src3*$^{-/-}$ mice (*n = 5* per genotype) and further expanded *in*

vitro for three days in the presence of $MOG_{35–55}$ and IL-23 (20 ng/ml). (**C**) Quantification of cells expressing characteristic mononuclear cell surface markers among CNS-infiltrating cells in host mice adoptively transferred with *Src3*$^{+/-}$ or *Src3*$^{-/-}$ $CD4^+$ T cells, assessed by flow cytometry at the peak of disease. (**D**) Gating strategy for lymphocytes shown in **C**. (**E**) qPCR analysis of *Il17a*, *Il17f*, *Csf2*, *Il22*, *Cxcr3*, and *Ccl20* mRNA in lymphocytes that infiltrated the CNS of mice (as in **B**). Expression is presented relative to that of the control gene *Actb*. Data are from three experiments (**A**, right panel, and **E**, presented as mean ± SEM; **C**, presented as median [central line], the first and third quartiles [box ends], and maximum and minimum [extended lines]). * $P < 0.05$ (*t-test*); ** $P < 0.01$ (*t-test*).

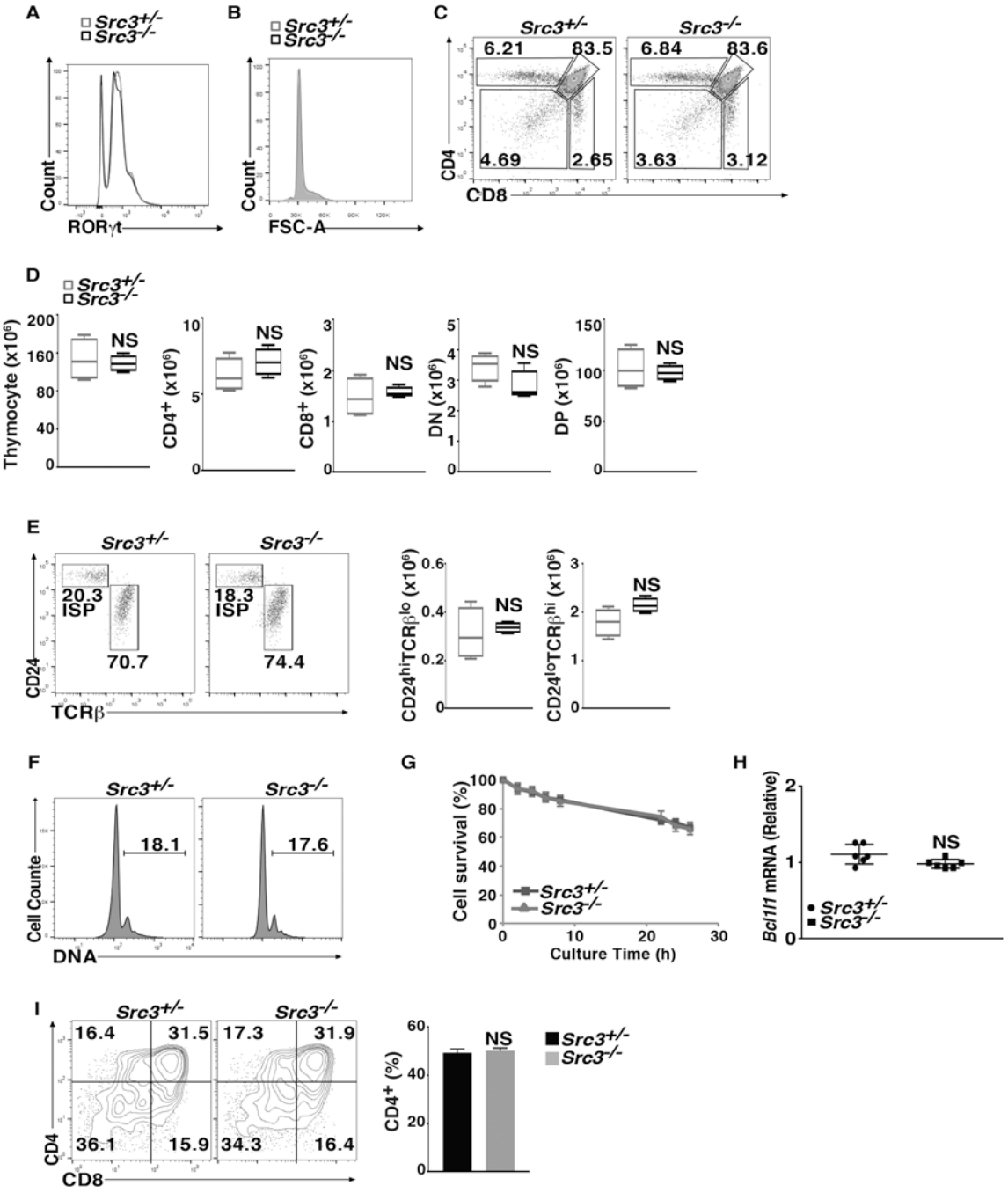

Figure 4.

SRC3 is not required for thymocyte development. (**A**) Flow cytometric analysis of RORγt expression among thymocytes in *Src3*$^{+/-}$ and *Src3*$^{-/-}$ mice. (**B**) Flow cytometric analysis of forward scatter (FSC-A) among thymocytes in *Src3*$^{+/-}$ and *Src3*$^{-/-}$ mice. (**C**) Flow cytometric analysis of CD4 and CD8 on the surface of *Src3*$^{+/-}$ and *Src3*$^{-/-}$ thymocytes. (**D**) Quantification of total thymocytes and CD4^{+}, CD8^{+}, CD4^{-}CD8^{-} double negative (DN), and CD4^{+}CD8^{+} double positive (DP) thymocytes of *Src3*$^{+/-}$ and *Src3*$^{-/-}$ mice (*n = 5* per genotype). (**E**) Flow cytometric analysis of CD24 and TCRβ expression in CD8^{+} cells

shown in **C** to assess the maturity of $CD8^+$ thymocytes (two panels on the left) and quantification of immature $TCR^{lo}CD24^{hi}$ and mature $TCR^{hi}CD24^{lo}$ cells (two panels on the right) (*n = 5* per genotype). (**F**) Flow cytometric analysis of DNA content (as 7-AAD staining) of $Src3^{+/-}$ and $Src3^{-/-}$ thymocytes. The numbers in each plot indicate the percentage of cells with >2N DNA. (**G**) Percentage of surviving cells among thymocytes obtained from $Src3^{+/-}$ and $Src3^{-/-}$ mice (*n = 5* per genotype) cultured for 0–15 h, then stained for the apoptosis marker annexin V and the membrane-impermeable DNA-interacting dye 7-AAD, analyzed by flow cytometry. (**H**) qPCR analysis of *Bcl2l1* mRNA in thymocytes from $Src3^{+/-}$ and $Src3^{-/-}$ mice (*n = 6* per genotype). (**I**) Flow cytometric analysis of CD4 and CD8 in cells differentiated from sorted $Src3^{+/-}$ and $Src3^{-/-}$ $CD4^-CD8^-$ thymocytes co-cultured for three days with OP9-DL4 cells in the presence of IL-7 (5 ng/ml) to assess *ex vivo* thymocyte development (left two panels). The plot on the right shows the percentages of $CD4^+$ plus $CD4^+CD8^+$ cells in each group. Data are from one representative of three independent experiments (**A-C**; **F**; **E** and **I,** left panel) or are aggregated from three experiments (**D**; **G**; **H**; **E** and **I**, right panels, presented as median [central line], maximum and minimum [box ends], and outliers [extended lines] or mean ± SEM). NS, not significant ($P>0.05$).

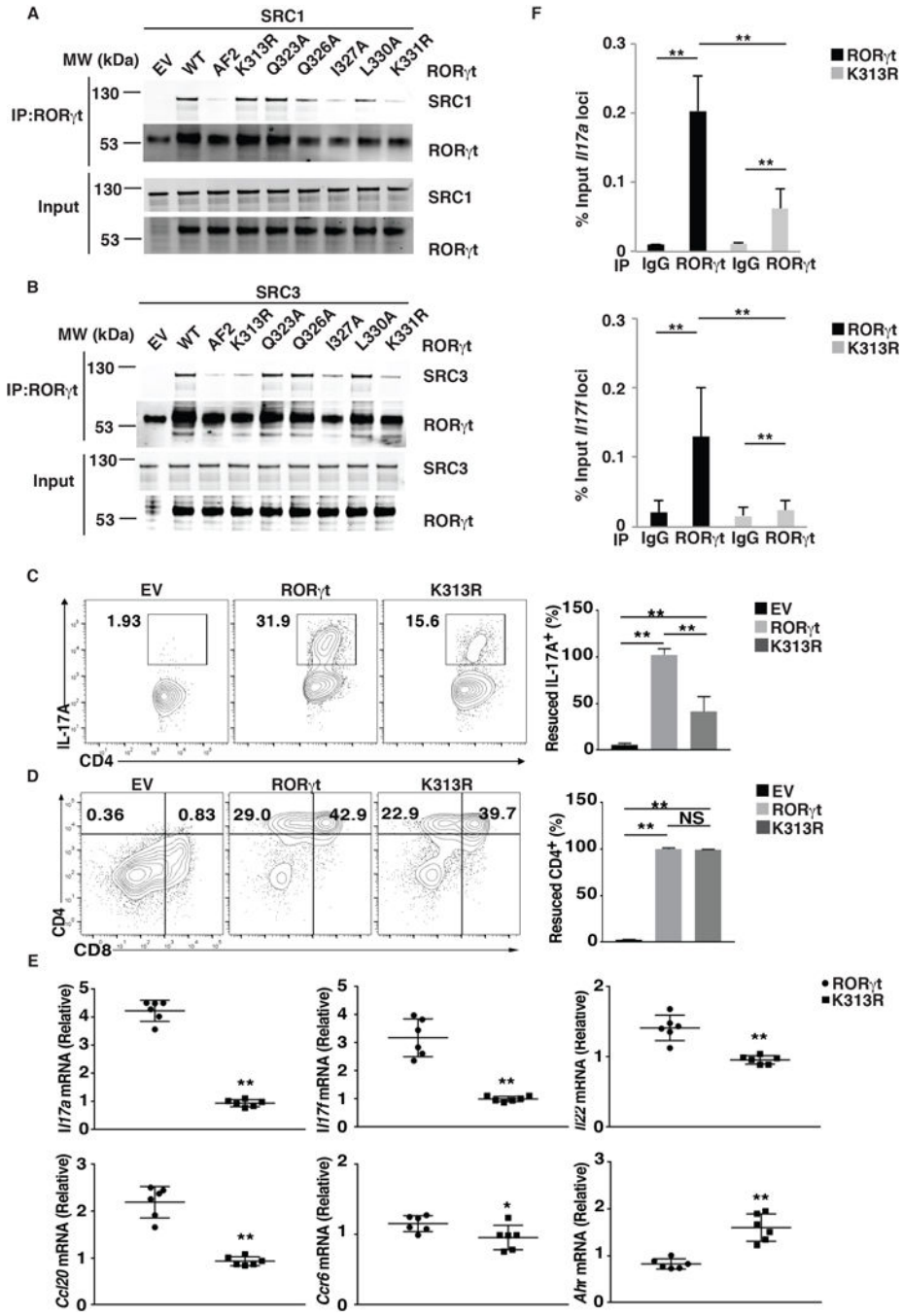

Figure 5.

Disruption of the RORγt-SRC3 interaction impairs the function of RORγt in Th17 differentiation but not in thymocyte development. (**A–B**) Immunoblot analysis of indicated SRC immunoprecipitated with an anti-RORγt antibody from HEK293T cells co-transfected with plasmids to express WT or mutant RORγt and (**A**) SRC1 or (**B**) SRC3. (**C**) Flow cytometric analysis of the percentage of IL-17A$^+$ cells (outlined) among *Rorγt*$^{-/-}$ CD4$^+$ T cells transduced with a retrovirus expressing GFP alone (EV) or GFP with wild-type RORγ or the RORγt-K313R mutant and polarized for three days under Th17 priming conditions.

The plot on the right shows the percentage of IL-17A$^+$ cells in each group. (**D**) Flow cytometric analysis of CD4 and CD8 in cells differentiated from *Rorγt*$^{-/-}$ CD4$^-$CD8$^-$ thymocytes transduced with a retrovirus expressing GFP alone (EV) or GFP with WT RORγ or RORγt-K313R and co-cultured for three days with OP9-DL4 cells in the presence of IL-7 (5 ng/ml) to assess *ex vivo* thymocyte development (left panels). The plot on the right shows the percentages of rescued CD4$^+$ plus CD4$^+$CD8$^+$ cells in each group. (**E**) qPCR analysis of mRNA of *Il17a, Il17f, Il22, Ccl20, Ccr6,* and *Ahr* in *Rorγt*$^{-/-}$ CD4$^+$ T cells transduced with WT RORγ (RORγ) or RORγt-K313R and polarized for three days under Th17 priming conditions, as shown in **C**. (**F**) ChIP analysis of RORγ or RORγt-K313R bound to *Il17a* (top panel) or *Il17f* (bottom panel) loci using *Rorγt*$^{-/-}$ CD4$^+$ T cells transduced with WT RORγ or the RORγt-K313R mutant and polarized for three days under Th17 priming conditions, as shown in **C.** Data are from one representative of three independent experiments (**A–B**; **C–D**, left panel) or are aggregated from three experiments (**C–D**, right panels; **E–F**, presented as mean ± SEM). NS, not significant (P>0.05); * P < 0.05 (*t-test*); ** P <0.01 (*t-test*).